

Reducing the Cost of Cycle-Time Tuning for Real-World Policy Optimization

Homayoon Farrahi

Department of Computing Science
University of Alberta
Edmonton, Canada
farrahi@ualberta.ca

A. Rupam Mahmood

Department of Computing Science
University of Alberta
Edmonton, Canada
armahmood@ualberta.ca

Abstract—Continuous-time reinforcement learning tasks commonly use discrete steps of fixed cycle times for actions. As practitioners need to choose the action-cycle time for a given task, a significant concern is whether the hyper-parameters of the learning algorithm need to be re-tuned for each choice of the cycle time, which is prohibitive for real-world robotics. In this work, we investigate the widely-used *baseline* hyper-parameter values of two policy gradient algorithms—PPO and SAC—across different cycle times. Using a benchmark task where the baseline hyper-parameters of both algorithms were shown to work well, we reveal that when a cycle time different than the task default is chosen, PPO with baseline hyper-parameters fails to learn. Moreover, both PPO and SAC with their baseline hyper-parameters perform substantially worse than their tuned values for each cycle time. We propose novel approaches for setting these hyper-parameters based on the cycle time. In our experiments on simulated and real-world robotic tasks, the proposed approaches performed at least as well as the baseline hyper-parameters, with significantly better performance for most choices of the cycle time, and did not result in learning failure for any cycle time. Hyper-parameter tuning still remains a significant barrier for real-world robotics, as our approaches require some initial tuning on a new task, even though it is negligible compared to an extensive tuning for each cycle time. Our approach requires no additional tuning after the cycle time is changed for a given task and is a step toward avoiding extensive and costly hyper-parameter tuning for real-world policy optimization.

I. INTRODUCTION

Continuous control with policy gradient methods in deep reinforcement learning (RL) has emerged as a promising approach to robot learning. However, except some recent works (Haarnoja et al. 2018b, Mahmood et al. 2018, Gupta et al. 2021), much of the advancements in this area rely on learning solely in simulations (Tan et al. 2018, Akkaya et al. 2019). Learning to control directly using physical robots remains a challenge due to many barriers such as sample inefficiency, partial observability, and delays in a real-time environment (Dulac-Arnold et al. 2021).

An oft-ignored issue of real-world RL is that, in a new physical environment, a choice regarding time discretization has to be made explicitly, whereas in simulated benchmark environments this choice is already made. In RL tasks, the

continuous time is typically discretized into steps of an equal duration called the *action-cycle time*, which refers to the time elapsed between two consecutive actions. In benchmark simulated environments, such as OpenAI Gym (Brockman et al. 2016) and DeepMind Control Suite (Tassa et al. 2020), the action-cycle time is usually already chosen to a suitable value for learning, and the choice of action-cycle time is not exposed as a subject of study. As a consequence, there is an absence of thorough investigations on how the existing algorithms perform across different cycle times.

When practitioners apply an RL algorithm to a new physical robotic task and need to tune the value of the action-cycle time for that task, a significant concern is how to choose the hyper-parameters of the algorithm. Tuning hyper-parameters for real-world tasks is difficult but not unprecedented (Mahmood et al. 2018). However, as a practitioner searches for a suitable cycle time, tuning the hyper-parameters for each choice of the cycle time becomes prohibitive. It will be of substantial advantage if the values of the hyper-parameters could be chosen robustly for all cycle times or adjusted based on the cycle time without re-tuning.

In this work, we study the hyper-parameters of two policy gradient methods called *Proximal Policy Optimization* (PPO, Schulman et al. 2017) and *Soft Actor-Critic* (SAC, Haarnoja et al. 2018a) across different cycle times. These two methods have been shown to perform effectively on many simulated benchmark tasks (Keng et al. 2019) and used for comparisons and further improvements in many other works (Fujimoto et al. 2018, Raffin & Stulp 2020) without extensive hyper-parameter tuning. In those works, roughly the same sets of hyper-parameter values are used separately for these two methods. These baseline hyper-parameter values are from the original works introducing the methods, and similar values are also used as the default values in widely-available implementations.

Our experiments on a widely-used benchmark simulation show that the baseline hyper-parameter values learn effectively with the default cycle time of the environment. However, when the cycle time changes, the baseline values of PPO fail to learn. Moreover, both PPO and SAC with their baseline values perform substantially worse than their tuned values for each cycle time. We also find that their tuned hyper-parameter values are different for different cycle times. Therefore, the

The authors thank the Reinforcement Learning and Artificial Intelligence Laboratory, Alberta Machine Intelligence Institute, Canada CIFAR AI Chairs Program, and Kindred Inc. for their generous support.

only known approach left for cycle-time tuning is to re-tune the hyper-parameters for each cycle time.

To reduce the cost associated with cycle-time tuning, we propose new approaches for setting algorithm hyper-parameters that adapt to new cycle times without re-tuning (see also Farrahi 2021). Our proposed approaches perform at least as well as and for many cycle times substantially better than the baseline values. Hyper-parameter values set by our recommendations do not fail to learn at any cycle time we used whereas the baseline values do. Our approach requires an initial tuning to an arbitrary cycle time on a task to enable the transfer of hyper-parameter values to different cycle times on the same task. Although an initial tuning is still needed, it is a strict improvement over extensive tuning for every new cycle time. Our approach therefore reduces the cost associated with hyper-parameter tuning when cycle time changes. We validate our recommendations on two held-out simulated and real-world robotic tasks. Our implementation of the tasks and experiments are publicly available at <https://github.com/homayoonfarrahi/cycle-time-study> to encourage future studies on cycle time.

II. RELATED WORK

Reducing the cycle time can inhibit effective learning in action-value methods. Baird (1994) illustrated that, at small cycle times, values of different actions in the same state get closer to each other, making learning the action-value function more sensitive to noise and function approximation error. They noted the collapse of the action-value function to the state-value function in continuous time and proposed the Advantage Updating algorithm. Their approach was later extended to deep Q -learning methods by Tallec et al. (2019). Policy gradient methods are also susceptible to degraded performance as cycle time gets smaller. The variance of likelihood-ratio policy gradient estimates can explode as cycle time goes toward zero as shown in an example by Munos (2006). They formulated a model-based policy gradient estimate assuming knowledge of the model and the gradient of the reward with respect to the state, which is hard to satisfy in many practical tasks. Based on the Hamilton-Jacobi-Bellman (HJB) equation, Doya (2000) derived the continuous-time TD error for learning the value function and extended the actor-critic method to continuous time. Lee and Sutton (2021) developed the theory for applying policy iteration methods to continuous-time systems.

The time it takes for an agent to output an action after an observation—the action delay—is particularly important in real-world robotics since, unlike simulations (Firoiu et al. 2018), real-world environments do not halt their progress as the agent calculates an action (Chen et al. 2021). Travnik et al. (2018) minimized action delay by reordering algorithmic steps. Dulac-Arnold et al. (2021) observed deteriorating performance with increasing action and observation delay. Ramstedt and Pal (2019) introduced the Real-Time Markov decision process and Actor-Critic in which cycle time should ideally be equal to the time for a forward pass of the policy, which could vary greatly for different policy architectures. In this work,

Algorithm 1: Agent-environment interaction loop for different cycle times

```

 $\Psi \doteq \text{Initialize}()$ 
Retrieve from  $\Psi$ : action-cycle time  $\delta t$ , environment
time step  $\delta t_{\text{env}}$ , learning period  $U$ , batch size  $b$ ,
parameterized policy  $\pi_{\theta}(a|s)$ 

Initialize Buffer  $B$  with capacity  $b$ 
Initialize  $S_0 \sim d_0(\cdot)$ 
 $j \doteq 0$  // episode step
 $k \doteq 0$  // agent step
for environment step  $i = 0, 1, 2, \dots$  do
  if  $j \bmod \delta t / \delta t_{\text{env}} = 0$  then
     $\tilde{S}_k \doteq S_i$ 
     $\tilde{R}_{k+1} \doteq 0$ 
    Calculate action  $\tilde{A}_k \sim \pi_{\theta}(\cdot|S_i)$ 
    Apply  $\tilde{A}_k$  and observe  $R_{i+1}, S'_{i+1}$ 
     $\tilde{R}_{k+1} \doteq \tilde{R}_{k+1} + R_{i+1}$ 
     $T_{i+1} \doteq \mathbb{1}_{S'_{i+1} \text{ is terminal}}$ 
  if  $j + 1 \bmod \delta t / \delta t_{\text{env}} = 0$  or  $T_{i+1} = 1$  then
    Store transaction in buffer
     $B_k = (\tilde{S}_k, \tilde{A}_k, \tilde{R}_{k+1}, S'_{i+1}, T_{i+1})$ 
  if  $k + 1 \bmod U = 0$  then
     $\Psi \doteq \text{Learn}(B, \Psi)$ 
     $k \doteq k + 1$ 
   $j \doteq j + 1$ 
  if  $T_{i+1} = 1$  then
    Sample  $S_{i+1} \sim d_0(\cdot)$ 
     $j \doteq 0$ 
  else
     $S_{i+1} \doteq S'_{i+1}$ 
end

```

we focus on the cycle time issues and assume that the chosen cycle times always fit the forward pass for action calculations. Dulac-Arnold et al. (2021) showed that increasing cycle time hurts task performance when using fixed hyper-parameters. The same can be true when reducing cycle time with fixed hyper-parameter values as we will show later.

III. THE PROBLEM SETUP

We use the undiscounted episodic reinforcement learning framework (Sutton & Barto 2018), which is a special case of discounted episodic Markov Decision processes (MDPs). In discounted episodic MDPs, an agent interacts with the environment through a sequence of episodes. Each episode starts with a state S_0 drawn from density d_0 . At time step t , the agent takes action A_t at state S_t and receives next state S_{t+1} and reward R_{t+1} until termination.

In this framework, the episodic return is denoted by $G_0 \doteq \sum_{k=0}^{T-1} \gamma^k R_{k+1}$ with the discount factor $\gamma \in [0, 1]$. The value of a state s under policy π is defined as $v_{\pi}(s) \doteq \mathbb{E}_{\pi} [G_0 | S_0 = s]$. When the policy π is parameterized by θ , the goal of the agent is to change θ to maximize the expected value of the initial state $J^{\gamma}(\theta) \doteq \int_s d_0(s) v_{\pi_{\theta}}(s)$. In our

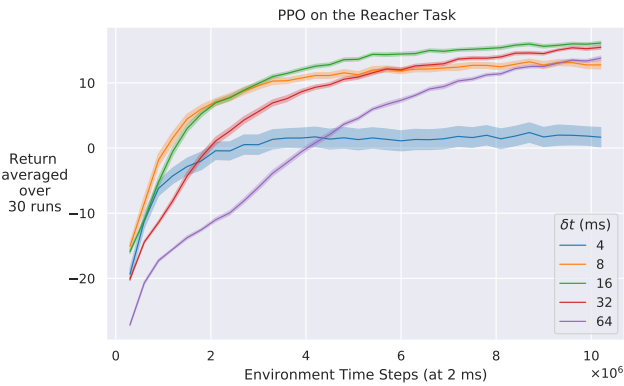


Fig. 1. Learning curves for the baseline PPO hyper-parameters under different cycle times δt . Smaller δt s have worse asymptotic performance. Larger δt s learn more slowly.

problem formulation, $\gamma = 1$, and we seek to maximize the expected undiscounted episodic return $J^1(\theta)$, although solution methods often use a surrogate objective with $\gamma < 1$.

Great care should be taken when running experiments with different cycle times in simulations. The naive approach of changing the time interval of the underlying physics engine for simulated environments may lead to inconsistencies between different cycle times since the environment can behave differently over time even if it receives the same sequence of actions for both cycle times. We instead run the environment at a small fixed environment time step δt_{env} , and simulate other cycle times as integer multiples of δt_{env} . Algorithm 1 describes the agent-environment interaction loop for this setup. This interaction loop is not specific to a particular learning algorithm, which can be instantiated by defining the *Initialize* and *Learn* functions as done in Appendix B for instance.

All parameters and hyper-parameters can be retrieved where needed from the set of all algorithm-specific parameters Ψ . The agent-environment interaction happens every $\delta t / \delta t_{\text{env}}$ environment steps, when the agent selects an action based on the latest environment state. The selected action \tilde{A}_k is repeatedly applied to the environment, and the received rewards are accumulated in \tilde{R}_{k+1} until the next action selection. Right before the next action selection, the transaction is stored in a buffer of size b , and the *Learn* function is executed if U agent-environment interactions have occurred. The buffer overwrites its oldest sample in case it is full. The two algorithms that we use for our experiments differ in their setting of batch size b and learning period U . In PPO (Appendix C), batch size b is equal to learning period U , whereas SAC (Appendix D) uses a much larger b than PPO with $U = 1$. In each call of the *Learn* function, PPO executes 10 epochs of mini-batch gradient updates, whereas SAC executes a single update.

IV. STUDYING THE BASELINE HYPER-PARAMETER VALUES OF PPO

In this section, we investigate the baseline hyper-parameter values of PPO across different cycle times. For our PPO

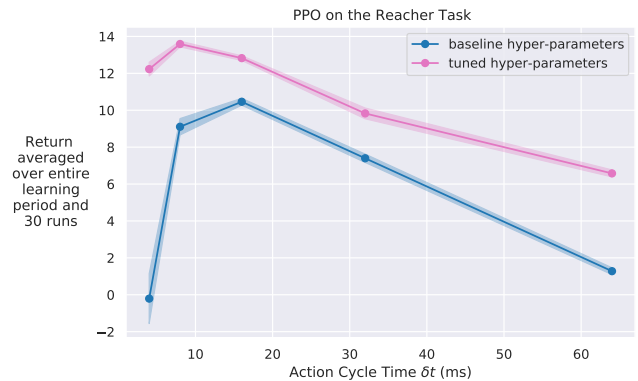


Fig. 2. Performance vs. cycle time δt for different hyper-parameter configurations of PPO. Tuned hyper-parameters improved the learning performance substantially for all δt s.

experiments in simulated environments, we use baseline hyper-parameter values similar to the recommended Mujoco hyper-parameters in Schulman et al. (2017). We use the PyBullet (Coumans & Bai 2016) environment *ReacherBulletEnv-v0* and refer to it as the *Reacher Task*. We modify its *environment time step* from the default 16.5ms to a constant 2ms for all experiments, and the agent interacts with the environment at multiples of 2ms for different cycle times. To run an experiment with cycle time $\delta t = 8\text{ms}$, for instance, the agent interacts with the environment every fourth environment step by taking the most recent observation as input and outputting an action, which is repeatedly applied to the environment until the next interaction. Rewards are accumulated between two interactions, and all episodes last for 2.4 seconds. Some components of the reward function are scaled according to the environment time step to keep their relative weighting comparable to the original environment.

We ran PPO with the baseline hyper-parameter values of Table I using various cycle times from 4ms to 64ms each for 10 million environment steps. The learning curve for each cycle time is given in Figure 1. We further performed a grid search with five different values of batch size from 500 to 8000 and mini-batch size from 12 to 200. For each set of hyper-parameters, average return over the entire learning period and 30 independent runs was calculated, and the results for the best-performing tuned hyper-parameter values at each cycle time (Table II) were plotted in Figure 2. We used separate runs to plot the results of the tuned hyper-parameter values to avoid maximization bias. Similar curve of average returns with fixed baseline hyper-parameter values was also plotted in Figure 2. For all plots in this paper, the results are calculated using undiscounted returns and shaded areas represent standard error.

Our experimental results in Figure 1 indicate that the baseline hyper-parameters can lead to learning failure when the cycle time changes, substantiated by the near zero return at 4ms, which does not give an effective goal-oriented behavior in this task. Figure 1 shows that the asymptotic performance declines with small cycle times and that large cycle times

hurt the learning speed. The former may be because batches are collected more quickly, lacking enough information for useful updates. The latter might be a result of fewer and infrequent updates. Figure 2 shows that tuning hyper-parameters to different values for each cycle time leads to substantially increased performance compared to the baselines. The tuned batch size and mini-batch size values are different from the baseline values and across cycle times. This demonstrates the importance of having guidelines for adjusting different hyper-parameters based on cycle time to allow transfer of hyper-parameters tuned to a specific cycle time to a different cycle time on the same task without re-tuning.

V. SETTING HYPER-PARAMETERS OF PPO AS A FUNCTION OF THE ACTION-CYCLE TIME

Changing the cycle time may affect the relationship between time, and the hyper-parameters batch size b and mini-batch size m , which could suggest the need for scaling them based on the cycle time. As the cycle time decreases, each fixed-size batch or mini-batch of samples corresponds to less amount of real-time experience, possibly reducing the extent of useful information available in the batch or mini-batch. To address this, we scale the baseline b and m inversely proportionally to the cycle time. Specifically, if $b_{\delta t_0}$ and $m_{\delta t_0}$ are the tuned or chosen batch size and mini-batch size, respectively, for the initial cycle time δt_0 (in ms), then the scaled batch size $b_{\delta t}$ and mini-batch size $m_{\delta t}$ for a new cycle time δt are as follows: $b_{\delta t} \doteq \frac{\delta t_0}{\delta t} b_{\delta t_0}$, $m_{\delta t} \doteq \frac{\delta t_0}{\delta t} m_{\delta t_0}$. For instance, reducing cycle time from the baseline $\delta t_0 = 16\text{ms}$ to 8ms , makes the batch size b_8 double the size of b_{16} . This keeps the *batch time* $\delta t \cdot b_{\delta t}$, the time it takes to collect a batch, and the amount of available information consistent across different cycle times.

The cycle time may influence the choice of the discount factor γ and the trace-decay parameter λ as well since it changes the rate at which rewards and n -step returns are discounted through time (Doya 2000, Tallec et al. 2019). When using a small cycle time, rewards and n -step returns are discounted more heavily for the same γ and λ , as more experience samples are collected in a fixed time interval compared to larger cycle times. Based on the above intuition discussed in previous works (Baird 1994, Doya 2000, Tallec et al. 2019), we exponentiated γ and λ to the $\delta t/\delta t_0$ power with initial cycle time δt_0 . However, this strategy was detrimental to the performance of smaller cycle times in our experiments perhaps since, as cycle time gets smaller, an increasing number of samples are used to calculate the likelihood-ratio policy gradient estimate, possibly leading to its increased variance (Munos 2006). Hence, we only exponentiate γ and λ to the $\delta t/\delta t_0$ power for cycle times larger than δt_0 . This can be achieved by setting $\gamma_{\delta t}$ and $\lambda_{\delta t}$ to be the minimum of the baseline and the scaled one. Based on the mentioned modifications, we present the new *δt -aware hyper-parameters* $b_{\delta t}$, $m_{\delta t}$, $\gamma_{\delta t}$ and $\lambda_{\delta t}$, which adapt to different cycle times as a function of the baseline action-cycle time δt_0 as follows: $b_{\delta t} \doteq \frac{\delta t_0}{\delta t} b_{\delta t_0}$, $m_{\delta t} \doteq \frac{\delta t_0}{\delta t} m_{\delta t_0}$, $\gamma_{\delta t} \doteq \min\left(\gamma_{\delta t_0}, \gamma_{\delta t_0}^{\delta t/\delta t_0}\right)$, and

$\lambda_{\delta t} \doteq \min\left(\lambda_{\delta t_0}, \lambda_{\delta t_0}^{\delta t/\delta t_0}\right)$. This proposed approach requires starting from a roughly tuned set of hyper-parameter values, which we call *the initial hyper-parameter values*, at an initially chosen cycle time δt_0 .

We evaluated the δt -aware hyper-parameters on the Reacher Task by setting the initial cycle time $\delta t_0 = 16\text{ms}$. The initial values of $m_{\delta t_0}$, $\gamma_{\delta t_0}$, and $\lambda_{\delta t_0}$ were set to the baseline values 50, 0.99, and 0.95 (Table III), respectively. We varied the initial batch size $b_{\delta t_0}$, which gives different initial hyper-parameter values, the overall performance of which for $\delta t_0 = 16\text{ms}$ is given by the green curve in Figure 3. For each choice of the initial hyper-parameter values, we calculated the δt -aware hyper-parameter values at different cycle times between 4ms and 64ms, and measured their overall performance, which are also given in Figure 3 with curves of different colors for different cycle times. With δt -aware hyper-parameter values, the curves aligned with each other well when the x-axis represents the batch time or the time it takes in seconds to collect a batch. A benefit of this alignment is that, if we tune the batch size at any initial cycle time, then for other cycle times the δt -aware hyper-parameters would give a batch size that performs the best within that cycle time, indicated by the vertical purple line, which signifies keeping the batch time fixed at the tuned initial value when changing the cycle time. For all cycle times, the δt -aware hyper-parameters calculated from PPO baselines (small solid-bordered circles at 32s batch time), performed better than the PPO baselines (dash-bordered circles). We also experimented with scaled batch and mini-batch sizes but γ and λ scaled without clipping. As shown in Figure 4, exponentiating γ and λ to the $\delta t/\delta t_0$ power reduces the performance of smaller cycle times for almost all batch times. Other cycle times looked exactly the same as in Figure 3 and were not drawn. When γ and λ were instead kept constant at the baseline values for all cycle times, larger cycle times performed worse (Figure 12).

VI. SETTING HYPER-PARAMETERS OF SAC AS A FUNCTION OF THE ACTION-CYCLE TIME

In this section, we first examine how changing the cycle time influences the performance of SAC and then how scaling the discount factor γ based on cycle time affects the performance of different cycle times. On the Reacher Task, we ran SAC with the baseline hyper-parameter values given by Haarnoja et al. (2018a) for 500,000 environment steps, and all other experimental details remain as in the previous sections. Figure 5 shows the resulting learning curves for each cycle time, averaged over 30 independent runs. As evident, the smaller cycle times 4ms and 8ms undergo sharp drops in performance just as the agent starts using the learned policy, although they are able to recover and match the performance of other cycle times swiftly. The larger $\delta t = 64\text{ms}$ learns more slowly throughout and never quite exceeds the learned performance of any other cycle time.

We explained previously how changing the cycle time can cause the rewards to be discounted faster or slower through time if γ is kept constant. As such, we continued by studying

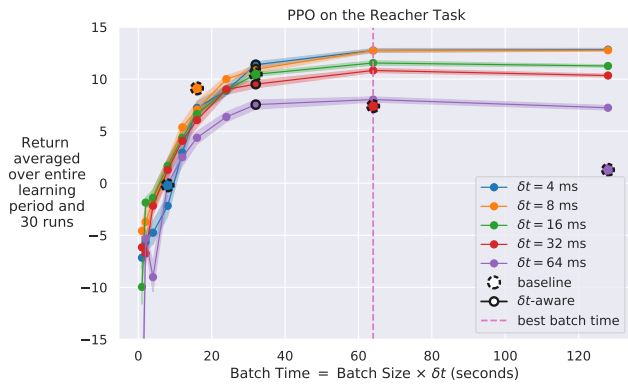


Fig. 3. Performance using the δt -aware hyper-parameters for different initial batch sizes. A close alignment of performance across different cycle times is obtained when batch time is kept constant.

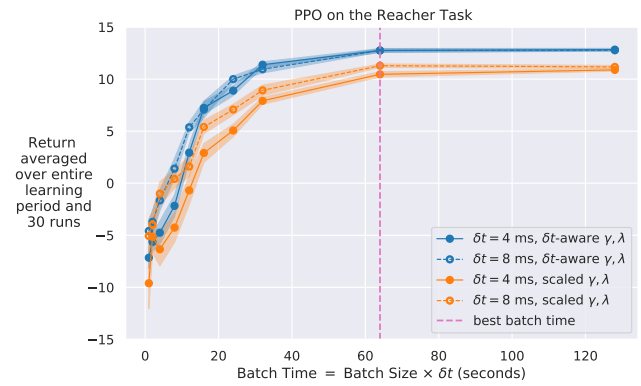


Fig. 4. Performance of δt -aware hyper-parameters for different initial batch sizes compared with ones where γ and λ are always exponentiated to the $\delta t/\delta t_0$ power (scaled).

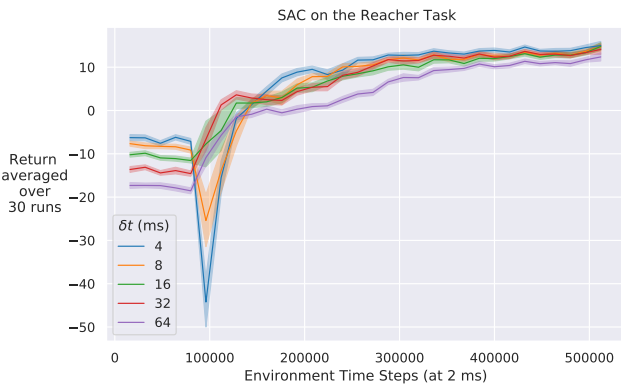


Fig. 5. Learning curves of baseline SAC hyper-parameters. Smaller cycle times suffer a sharp decline in the beginning, and the largest cycle time learns more slowly.

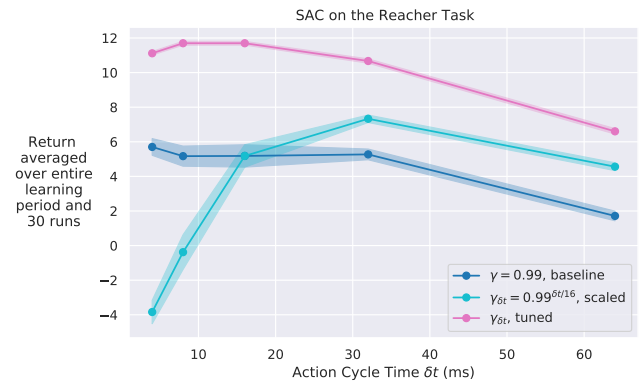


Fig. 6. Performance vs. cycle time for different choices of γ . Scaling γ based on cycle time makes the performance more sensitive to cycle time. Performance can be improved by tuning γ for each cycle time separately.

the effect of scaling and tuning the discount factor γ on performance. We scaled the discount factor for each cycle time according to $\gamma_{\delta t} = \gamma_{16}^{\delta t/16}$ with baseline $\gamma_{16} = 0.99$ to ensure consistent discounting of the rewards through time (Doya 2000, Tallec et al. 2019). Average returns over the entire learning period and 30 runs were plotted in Figure 6 (curve in cyan). Similar curves were drawn for two additional sets of experiments. In the first set, baseline hyper-parameter values including $\gamma = 0.99$ stayed constant across all cycle times (curve in blue). In the second set, the best $\gamma_{\delta t}$ was found by searching over 12 different values from $0.99^{1/28} = 0.2763$ to 1.0 for each cycle time individually and rerun to avoid maximization bias (curve in purple). Exponentiating the baseline γ to the $\delta t/16$ power surprisingly makes SAC more sensitive to cycle time, as it boosts the performance of larger cycle times and hinders that of smaller ones. Tuning γ to different values, however, can substantially improve the results of all cycle times over the baseline and scaled values. The tuned γ values (Table IV) are different from the baseline $\gamma = 0.99$ and across cycle times. Scaling γ was not a better choice than the baseline, and tuning γ outperformed both.

Figure 7 shows the average return of different γ s and cycle times to better illustrate the relationship between them. The best performance at $\delta t = 16$ ms is reached with $\gamma \approx 0.851$, which is considerably far from the baseline value of 0.99. The performance of all cycle times peak at different intermediate values of γ and steadily decline for both increasing and decreasing γ s (except for the curious jump of $\delta t = 4$ ms at the smallest γ). The location of these peaks might be different for other tasks with some tasks obtaining the maximum performance with γ s larger than the baseline 0.99. In this task, the baseline γ is larger than the best, and scaling it according to cycle time hurts the performance of smaller cycle times (solid-bordered circles in Figure 7). If the best γ was larger than the baseline instead, scaling it would have helped smaller cycle times. This conflict points to the insufficiency of merely scaling γ for adapting it to different cycle times. In addition, as cycle time gets larger, the curves are consistently stretched horizontally, which hints at the need for scaling γ based on cycle time to make the curves more aligned.

Based on the results of the exhaustive γ sweep, we propose two approaches for adapting γ to different cycle times. In

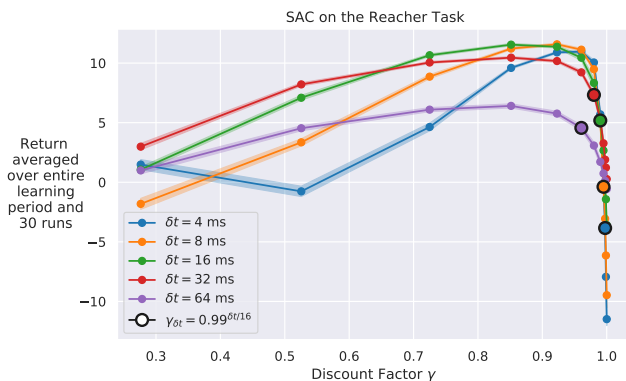


Fig. 7. Performance for a sweep of γ values. Peak performance is achieved at intermediate values of γ . Curves are stretched horizontally for increasing cycle time, suggesting the need for scaling γ based on cycle time.

the first approach, γ is initially tuned to find the best value at an initial δt_0 and subsequently scaled based on the cycle time. In the second approach, the tuned γ is kept constant for other cycle times. These two approaches are the new δt -aware discount factor $\gamma_{\delta t,1}$ and $\gamma_{\delta t,2}$ of SAC defined as $\gamma_{\delta t,1} \doteq (\arg\max_{\gamma_{\delta t_0}} \hat{G}_0)^{\delta t/\delta t_0}$ $\gamma_{\delta t,2} \doteq (\arg\max_{\gamma_{\delta t_0}} \hat{G}_0)$ with δt_0 as the initial cycle time and \hat{G}_0 as the estimate of the undiscounted episodic return obtained as a sample average over the entire learning process. We tested the two approaches for the δt -aware $\gamma_{\delta t}$ on the Reacher Task with $\delta t_0 = 16\text{ms}$, for which $\gamma_{16} \approx 0.851$ performed best. Figure 8 (left) shows that both of these approaches performed significantly better than the baseline $\gamma = 0.99$. It is thus clear that tuning γ for SAC at δt_0 is a crucial step in adapting it to different cycle times. The additional scaling in $\gamma_{\delta t,1}$ benefits smaller cycle times and hurts larger ones.

VII. VALIDATING THE δt -AWARE HYPER-PARAMETERS ON A HELD-OUT SIMULATED TASK

In this section, we validate our proposed δt -aware hyper-parameters on the PyBullet environment *InvertedDoublePendulumBulletEnv-v0* referred to as the *Double Pendulum Task*. We reduced the environment time step from 16.5ms to a constant 4ms. Episodes lasted a maximum of 16 simulation seconds. We ran two sets of experiments with PPO. For the first set, we kept the baseline hyper-parameters ($b = 2000$) constant across cycle times, and for the second set, we used the δt -aware hyper-parameters of Table III with $\delta t_0 = 16\text{ms}$ ($b_{16} = 2000$) and initial values set to the baselines. All runs lasted for 10 million environment steps, and the average returns over the full learning period were plotted in Figure 8 (middle). We investigated the validity of both approaches for $\gamma_{\delta t}$ of SAC on the Double Pendulum Task and compared them with the baseline $\gamma = 0.99$. Peak performance at $\delta t_0 = 16\text{ms}$ was achieved with $\gamma = 0.9987$, which was both held constant across and scaled based on different cycle times. All runs lasted for one million

environment steps with results depicted in Figure 8 (right). Other experimental details were similar to previous sections.

For both PPO and SAC, the δt -aware hyper-parameters were an improvement over the baseline values and did not fail to learn at any cycle time, as opposed to the ineffective performance of baseline values at $\delta t = 4\text{ms}$, which was confirmed by rendering the behavior after learning. Figure 8 (right) validates $\gamma_{\delta t}$ of SAC, as the requisite tuning of γ done by $\gamma_{\delta t,2}$ at an initial δt_0 retrieved the lost performance at smaller cycle times with only marginal refinement resulting from the subsequent scaling done by $\gamma_{\delta t,1}$. Contrary to the baselines, the δt -aware hyper-parameters did not fail to learn at any cycle time. The baseline $\gamma = 0.99$ particularly impairs the performance of $\delta t = 4$ and $\delta t = 8\text{ms}$, which contrasts the outcomes from the Reacher Task shown in Figure 8 (left). The baseline value of γ in the SAC algorithm, therefore, may not be effective across different environments and cycle times, which remains an issue for future studies.

VIII. VALIDATION ON A REAL-WORLD ROBOTIC TASK

We validated the δt -aware hyper-parameters of PPO and SAC on the *UR-Reacher-2* task shown in Figure 9 developed by Mahmood et al. (2018), which we call the *Real-Robot Reacher Task*. We set the environment time step to 10ms. Three sets of experiments were run using PPO. In the first set, we used $\delta t_0 = 40\text{ms}$ as the benchmark. The other two sets used $\delta t = 10\text{ms}$ to compare baseline initial hyper-parameter values ($b = 400$, $m = 10$, $\gamma = 0.99$, $\lambda = 0.95$), kept constant across cycle times, to the δt -aware hyper-parameters that adapt to $\delta t = 10\text{ms}$, e.g., $b_{10} = \frac{\delta t_0}{10} b_{\delta t_0} = \frac{40}{10} \times 400 = 1600$. The baseline values were chosen since they perform well on this task at $\delta t_0 = 40$. All episodes were 4 seconds long for all cycle times. Each run lasted for 600,000 environment steps or 100 real-time minutes, and the learning curves, averaged over five runs, were plotted in Figure 10. For SAC, the environment time step was set to 40ms to ensure the learning updates take no longer than a cycle time. A $\gamma \approx 0.9227$ produced peak performance at $\delta t_0 = 40\text{ms}$. Three sets of experiments at $\delta t = 120\text{ms}$ were performed using the baseline $\gamma = 0.99$, the tuned $\gamma_{\delta t,2} \approx 0.9227$, and the tuned and scaled $\gamma_{\delta t,1} \approx 0.9227^{120/40} = 0.786$. Figure 11 shows the returns averaged over 10 independent runs and 50,000 environment steps or 33 real-time minutes for each set of experiments. The learning curves for $\delta t = 40\text{ms}$ and $\delta t = 120\text{ms}$ are in Figures 25 and 26, respectively. Videos of the learned policies can be seen at <https://www.youtube.com/watch?v=tmo5fWGRPtK>.

As seen in Figure 10, the δt -aware hyper-parameters of PPO on Real-Robot Reacher recovered the lost performance of baseline hyper-parameter values with a small cycle time. The δt -aware hyper-parameters of PPO at $\delta t = 10\text{ms}$ achieved an asymptotic performance similar to or slightly better than the baselines at $\delta t_0 = 40\text{ms}$, whereas the baselines performed significantly worse at $\delta t = 10\text{ms}$. The performances of $\delta t = 10\text{ms}$ and $\delta t_0 = 40\text{ms}$ were comparable with the Mujoco baseline values ($b = 2000$) of Table III (Figure 24). For the SAC experiments in Figure 11, the baseline $\gamma = 0.99$ reduced

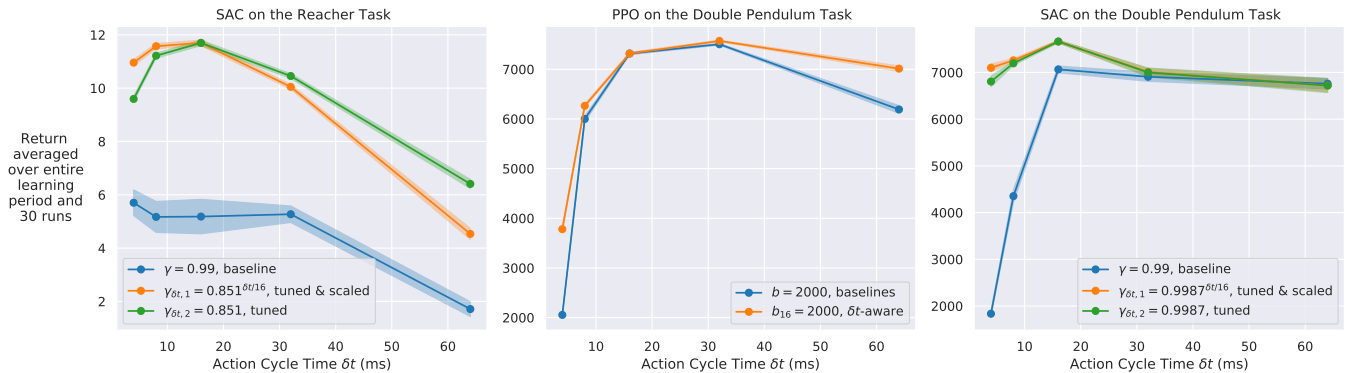


Fig. 8. (left) Performance of the two hypotheses compared with baseline γ . Both offer notable performance gains over the baseline. Scaling γ according to cycle time favors smaller cycle times and hurts larger ones. (middle) Performance of δt -aware and baseline hyper-parameters compared. The δt -aware values improve over the baselines and do not fail to learn at $\delta t = 4$ ms. (right) Performance of δt -aware $\gamma_{\delta t}$ of SAC compared with baseline γ . The tuned $\gamma_{\delta t,2}$ fully regains the performance of smaller cycle times. Additional scaling ($\gamma_{\delta t,1}$) causes only a marginal refinement.

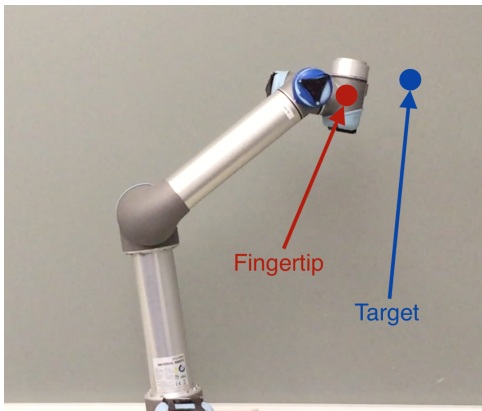


Fig. 9. Real-Robot Reacher Task. The goal is to move the base and elbow joints to get the fingertip as close to target as fast as possible.

the performance when cycle time changed from 40ms to 120ms. Using the tuned $\gamma_{\delta t,2} \approx 0.9227$ provided a modest recovery, and the additional scaling based on cycle time regained a performance almost similar to the peak at $\delta t_0 = 40$ ms. The results indicate that tuning γ for an initial δt_0 is essential for adapting γ to different cycle times. The high performance of $\delta t = 120$ ms with an atypical $\gamma_{\delta t,1} \approx 0.9227^{120/40} = 0.786$ demonstrates the necessity of having guidelines such as our δt -aware $\gamma_{\delta t}$ to avoid the poor performance of the baseline $\gamma = 0.99$ when changing the cycle time, especially since we observed that the asymptotic performance of $\gamma = 0.99$ at $\delta t = 120$ ms remains lower than the peak even after extended learning. Our δt -aware hyper-parameters can thus lessen the demand for costly hyper-parameter tuning in the real world.

IX. CONCLUSIONS

We introduced three benchmark tasks modified from existing tasks for cycle-time study and demonstrated that PPO may fail to learn using the baseline hyper-parameter values when the cycle time changes. Baseline hyper-parameter values performed significantly worse than their tuned values for both

PPO and SAC. We proposed a replacement set of δt -aware hyper-parameters that adapt to different cycle times, and empirically showed that they perform as well as or substantially better than the baseline ones without re-tuning. As opposed to the baseline hyper-parameters, the δt -aware ones did not fail to learn with any cycle time. Our δt -aware hyper-parameters can transfer hyper-parameter values tuned to a particular cycle time to different cycle times on the same task without re-tuning and can lessen the need for extensive hyper-parameter tuning when cycle time changes for both PPO and SAC, which is time-consuming and costly on real-world robots. We finally validated the δt -aware hyper-parameters on simulated and real-world robotic tasks. Our extensive experiments amounted to 75 real-time hours or 10 million time steps of real-world robot learning, along with 20,000 and 1000 simulation hours for PPO and SAC respectively.

REFERENCES

- Akkaya, I., Andrychowicz, M., Chociej, M., Litwin, M., McGrew, B., Petron, A., Paino, A., Plappert, M., Powell, G., Ribas, R., Schneider, J., Tezak, N., Tworek, J., Welinder, P., Weng, L., Yuan, Q., Zaremba, W., Zhang, L. (2019). Solving rubik’s cube with a robot hand. *arXiv preprint arXiv:1910.07113*.
- Baird, L. C. (1994). Reinforcement learning in continuous time: Advantage updating. In *Proceedings of 1994 IEEE International Conference on Neural Networks*.
- Brockman, G., Cheung, V., Pettersson, L., Schneider, J., Schulman, J., Tang, J., Zaremba, W. (2016). Openai gym. *arXiv preprint arXiv:1606.01540*.
- Chen, B., Xu, M., Li, L., Zhao, D. (2021). Delay-aware model-based reinforcement learning for continuous control. *Neurocomputing* 450:119–128.
- Coumans, E., Bai, Y. (2016). PyBullet, a python module for physics simulation for games, robotics and machine learning. URL <http://pybullet.org>
- Doya, K. (2000). Reinforcement learning in continuous time and space. *Neural Computation* 12 (1):219–245.

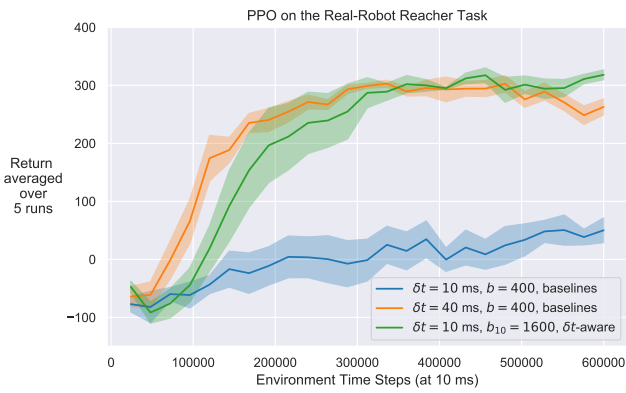


Fig. 10. Learning curves of PPO on the Real-Robot Reacher Task comparing the δt -aware hyper-parameters with the baseline ones. Asymptotic performance is recovered by the δt -aware hyper-parameters.

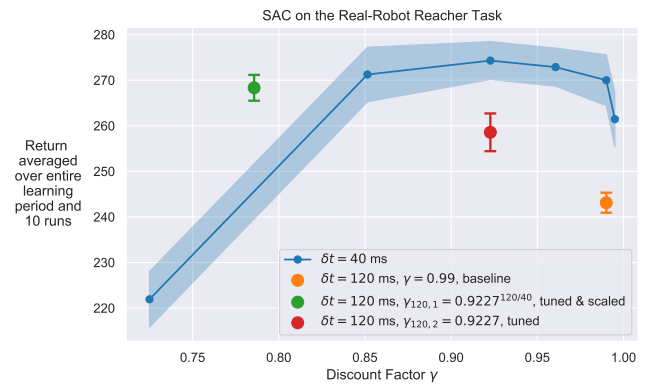


Fig. 11. Performance of SAC comparing the baseline γ with our two hypotheses on Real-Robot Reacher. The tuned and scaled $\gamma_{\delta t,1}$ almost fully recovers the poor performance of the baseline γ on $\delta t = 120$ ms.

Dulac-Arnold, G., Levine, N., Mankowitz, D. J., Li, J., Paduraru, C., Goyal, S., Hester, T. (2021). Challenges of real-world reinforcement learning: Definitions, benchmarks and analysis. *Machine Learning*. Advance online publication. <https://doi.org/10.1007/s10994-021-05961-4>.

Farrahi, H. (2021). Investigating two policy gradient methods under different time discretizations. Master's thesis, Department of Computing Science, University of Alberta, Edmonton, AB T6G 2E8.

Firoiu, V., Ju, T., Tenenbaum, J. (2018). At human speed: Deep reinforcement learning with action delay. *arXiv preprint arXiv:1810.07286*.

Fujimoto, S., Hoof, H., Meger, D. (2018). Addressing function approximation error in actor-critic methods. In *International Conference on Machine Learning*.

Gupta, A., Yu, J., Zhao, T. Z., Kumar, V., Rovinsky, A., Xu, K., Devlin, T., Levine, S. (2021). Reset-free reinforcement learning via multi-task learning: Learning dexterous manipulation behaviors without human intervention. In *2021 IEEE International Conference on Robotics and Automation*.

Haarnoja, T., Zhou, A., Hartikainen, K., Tucker, G., Ha, S., Tan, J., Kumar, V., Zhu, H., Gupta, A., Abbeel, P., Levine, S. (2018a). Soft actor-critic algorithms and applications. *arXiv preprint arXiv:1812.05905*.

Haarnoja, T., Ha, S., Zhou, A., Tan, J., Tucker, G., Levine, S. (2018b). Learning to walk via deep reinforcement learning. In *Robotics: Science and Systems XV*.

Keng, W. L., Graesser, L., Cvitkovic, M. (2019). SLM lab: A comprehensive benchmark and modular software framework for reproducible deep reinforcement learning. *arXiv preprint arXiv:1912.12482*.

Kingma, D. P., Ba, J. (2014). Adam: A method for stochastic optimization. In *3rd International Conference on Learning Representations*.

Lee, J., Sutton, R. S. (2021). Policy iterations for reinforcement learning problems in continuous time and space—fundamental theory and methods. *Automatica* 126, Article 109421.

Mahmood, A. R., Korenkevych, D., Vasan, G., Ma, W., Bergstra, J. (2018). Benchmarking reinforcement learning algorithms on real-world robots. In *Proceedings of the 2nd Annual Conference on Robot Learning*.

Munos, R. (2006). Policy gradient in continuous time. *Journal of Machine Learning Research* 7 (27):771–791.

Raffin, A., Stulp, F. (2020). Generalized state-dependent exploration for deep reinforcement learning in robotics. *arXiv preprint arXiv:2005.05719*.

Ramstedt, S., Pal, C. (2019). Real-time reinforcement learning. In *Advances in Neural Information Processing Systems*.

Schulman, J., Wolski, F., Dhariwal, P., Radford, A., Klimov, O. (2017). Proximal policy optimization algorithms. *arXiv preprint arXiv:1707.06347*.

Sutton, R. S., Barto, A. G. (2018). *Reinforcement Learning: An Introduction*. MIT Press.

Tallec, C., Blier, L., Ollivier, Y. (2019). Making deep Q-learning methods robust to time discretization. In *Proceedings of the 36th International Conference on Machine Learning*.

Tan, J., Zhang, T., Coumans, E., Iscen, A., Bai, Y., Hafner, D., Bohez, S., Vanhoucke, V. (2018). Sim-to-real: Learning agile locomotion for quadruped robots. *arXiv preprint arXiv:1804.10332*.

Tassa, Y., Tunyasuvunakool, S., Muldal, A., Doron, Y., Trochim, P., Liu, S., Bohez, S., Merel, J., Erez, T., Lillicrap, T., Heess, N. (2020). dm_control: Software and tasks for continuous control. *arXiv preprint arXiv:2006.12983*.

Travnik, J. B., Mathewson, K. W., Sutton, R. S., Pilarski, P. M. (2018). Reactive reinforcement learning in asynchronous environments. *Frontiers in Robotics and AI* 5:79.

APPENDIX
ALGORITHMS

A. The Standard Agent-Environment Interaction Loop

Algorithm 2: Agent-environment interaction loop

```

Ψ ≐ Initialize()
Retrieve from Ψ: learning period U, batch size b,
parameterized policy πθ(a|s)
Initialize Buffer B with capacity b
Initialize S0 ~ d0(·)
for environment step i = 0, 1, 2, ... do
  Calculate action Ai ~ πθ(·|Si)
  Apply Ai and observe Ri+1, S'_{i+1}
  Ti+1 ≐ 1_{S'_{i+1} is terminal}
  Store transaction in buffer
  Bi = (Si, Ai, Ri+1, S'_{i+1}, Ti+1)
  if i + 1 mod U = 0 then
    Ψ ≐ Learn(B, Ψ)
  if Ti+1 = 1 then
    Sample Si+1 ~ d0(·)
  else
    Si+1 ≐ S'_{i+1}
end

```

B. One-Step Actor-Critic

Algorithm 3: One-step actor-critic Initialize and Learn functions

```

Function Initialize():
  Ψ ≐ { learning period U, batch size b, discount
  factor γ, parameterized policy πθ(a|s),
  parameterized value estimate  $\hat{v}_{\mathbf{w}}(s)$ , current
  discount I, policy learning rate ηθ, value estimate
  learning rate ηw }

  Denote network parameters by Ψ.θ, and Ψ.w
  Initialize parameters Ψ.θ, Ψ.w
  I ≐ 1
  return Ψ

Function Learn(B, Ψ):
  Retrieve the only transaction in the buffer
  St, At, Rt+1, S'_{t+1}, Tt+1
  θ ≐ Ψ.θ ; w ≐ Ψ.w
   $\bar{\mathbf{w}} \doteq \mathbf{w}$ 
  δt ≐ Rt+1 + (1 - Tt+1)γ $\hat{v}_{\bar{\mathbf{w}}}(S'_{t+1})$  -  $\hat{v}_{\mathbf{w}}(S_t)$ 
  θ ≐ θ + ηθIδt∇θ log πθ(At|St)
  w ≐ w + ηwIδt∇w $\hat{v}_{\mathbf{w}}(S_t)$ 
  if Tt+1 = 1 then I ≐ 1
  else I ≐ γI
  Ψ.θ ≐ θ ; Ψ.w ≐ w
  return Ψ

```

C. Proximal Policy Optimization

Algorithm 4 shows the *Initialize* and *Learn* functions of PPO. Hyper-parameters $N = 10$ and $\epsilon = 0.2$ remained fixed across all experiments. Batch size and the learning period were always equal $b = U$. We used the Adam optimizer (Kingma & Ba 2014) with the same learning rate of 0.0003 for both policy and value estimate objectives. The architecture of the agent comprises a neural network of two hidden layers, each with 64 units and tanh activations, producing the mean μ , and state-independent parameters for the σ of a normal distribution $\mathcal{N}(\mu, \sigma^2)$ from which the actions are sampled. The value estimate is parameterized by another neural network configured similarly to that which produces μ . The equation below shows the gradient of the policy objective that is used in the algorithm.

$$\nabla_{\theta} L_{\theta, t} = \begin{cases} -\frac{\nabla_{\theta} \pi_{\theta}(A_t|S_t)}{\pi_{\theta_{old}}(A_t|S_t)} \tilde{h}_t, & \text{if } \rho_t(\theta) \tilde{h}_t \leq \rho_t^{\text{clip}}(\theta) \tilde{h}_t \\ & \text{or } \left(\rho_t(\theta) \tilde{h}_t > \rho_t^{\text{clip}}(\theta) \tilde{h}_t \text{ and } \right. \\ & \left. 1 - \epsilon \leq \rho_t(\theta) \leq 1 + \epsilon \right) \\ 0, & \text{otherwise} \end{cases} \quad (1)$$

Algorithm 4: PPO Initialize and Learn functions

Function Initialize():

$\Psi \doteq \{$ learning period U , number of epochs N ,
batch size b , mini-batch size m , discount factor γ ,
trace-decay parameter λ , clipping parameter ϵ ,
parameterized policy $\pi_{\theta}(a|s)$, parameterized value
estimate $\hat{v}_{\mathbf{w}}(s)$, learning rate η $\}$

Denote network parameters by $\Psi.\theta$, and $\Psi.\mathbf{w}$

Initialize parameters $\Psi.\theta$, $\Psi.\mathbf{w}$

return Ψ

Function Learn(B, Ψ):

$\theta \doteq \Psi.\theta$; $\mathbf{w} \doteq \Psi.\mathbf{w}$

$\bar{\mathbf{w}} \doteq \mathbf{w}$

for $t = 0, 1, 2, \dots, b$ **do**

Retrieve transaction from buffer

$S_t, A_t, R_{t+1}, S'_{t+1}, T_{t+1}$

$T \doteq \min \{j \mid j \in \mathbb{N} \wedge j > t \wedge T_j = 1\}$

$G_t^\lambda \doteq \lambda^{T-t-1} G_t + (1-\lambda) \sum_{n=1}^{T-t-1} \lambda^{n-1} G_{t:t+n}$,

where

$G_{t:t+n} \doteq \gamma^n \hat{v}_{\bar{\mathbf{w}}}(S_{t+n}) + \sum_{j=1}^n \gamma^{j-1} R_{t+j}$

$\hat{h}_t \doteq G_t^\lambda - \hat{v}_{\mathbf{w}}(S_t)$ // advantage
estimate

end

$\tilde{h} \doteq \text{normalize}(\hat{h})$

$D \doteq \left((S_t, A_t, \tilde{h}_t, G_t^\lambda) \right)_{t=0}^b$

$\theta_{old} \doteq \theta$

for epoch $e = 1, 2, \dots, N$ **do**

$\tilde{D} \doteq \text{shuffle}(D)$

Slice \tilde{D} into $\lceil \frac{b}{m} \rceil$ mini-batches

for each mini-batch M **do**

$\theta \doteq \theta - \eta \frac{1}{m} \sum_{(S_k, A_k, \tilde{h}_k) \in M} \nabla_{\theta} L_{\theta, k}$
using (1), where

$L_{\theta, k} \doteq - \min \left(\rho_k(\theta) \tilde{h}_k, \rho_k^{\text{clip}}(\theta) \tilde{h}_k \right)$,

$\rho_k(\theta) \doteq \frac{\pi_{\theta}(A_k|S_k)}{\pi_{\theta_{old}}(A_k|S_k)}$, and

$\rho_k^{\text{clip}}(\theta) \doteq \text{clip}(\rho_k(\theta), 1 - \epsilon, 1 + \epsilon)$

$\mathbf{w} \doteq \mathbf{w} +$

$\eta \frac{1}{m} \sum_{(S_k, G_k^\lambda) \in M} 2 (G_k^\lambda - \hat{v}_{\mathbf{w}}(S_k)) \nabla_{\mathbf{w}} \hat{v}_{\mathbf{w}}(S_k)$

end

end

$\Psi.\theta \doteq \theta$; $\Psi.\mathbf{w} \doteq \mathbf{w}$

return Ψ

D. Soft Actor-Critic

Algorithm 5 shows the *Initialize* and *Learn* functions of SAC. Hyper-parameters $b = 1,000,000$, $U = 1$, $m = 256$, $g = 1$, and $\tau = 0.005$ remained constant for all experiments. We used the Adam optimizer (Kingma & Ba 2014) for all objectives with learning rates set to 0.0003. Both the policy and the action-value estimates were parameterized using neural networks with two hidden layers of size 256 with ReLU activations. The hidden layers of the policy parameters were shared between mean μ and standard deviation σ of the normal distribution $\mathcal{N}(\mu, \sigma^2)$ that was used to draw the actions. Following equations are the gradients of all objectives that are used in the algorithm.

$$\begin{aligned} \nabla_{\theta} L_{\theta,t} = & \alpha \nabla_{\theta} \log \pi_{\theta}(a|S_t)|_{a=f(S_t, \epsilon_t, \theta)} \\ & + \nabla_{\theta} f(S_t, \epsilon_t, \theta) \left(\alpha \nabla_a \log \pi_{\theta}(a|S_t)|_{a=f(S_t, \epsilon_t, \theta)} \right. \\ & \left. - \nabla_a \hat{q}_{\mathbf{w}_{\min}}(S_t, a)|_{a=f(S_t, \epsilon_t, \theta)} \right), \text{ where} \end{aligned} \quad (2)$$

$$\mathbf{w}_{\min} \doteq \underset{\mathbf{w} \in \{\mathbf{w}_1, \mathbf{w}_2\}}{\operatorname{argmin}} \hat{q}_{\mathbf{w}}(S_t, f(S_t, \epsilon_t, \theta)),$$

$$\begin{aligned} \nabla_{\mathbf{w}_i} L_{\mathbf{w}_i,t} = & \left(\hat{q}_{\mathbf{w}_i}(S_t, A_t) - (R_{t+1} + (1 - T_{t+1})\gamma V(S'_{t+1})) \right) \\ & \nabla_{\mathbf{w}_i} \hat{q}_{\mathbf{w}_i}(S_t, A_t) \text{ for } i \in \{1, 2\}, \end{aligned} \quad (3)$$

$$\nabla_{\alpha} L_{\alpha,t} = -\log \pi_{\theta}(f(S_t, \epsilon_t, \theta)|S_t) - \bar{\mathcal{H}}. \quad (4)$$

Algorithm 5: SAC Initialize and Learn functions

Function Initialize():

$\Psi \doteq \{$ learning period U , batch size b , mini-batch size m , gradient steps g , discount factor γ , temperature parameter α , target smoothing coefficient τ , parameterized policy $\pi_{\theta}(a|s)$, policy mean $\mu_{\theta}(s)$, policy standard deviation $\sigma_{\theta}(s)$, parameterized action-value estimates $\hat{q}_{\mathbf{w}_1}(s, a)$, $\hat{q}_{\mathbf{w}_2}(s, a)$, $\hat{q}_{\bar{\mathbf{w}}_1}(s, a)$, $\hat{q}_{\bar{\mathbf{w}}_2}(s, a)$, policy learning rate η^{θ} , action-value estimate learning rate $\eta^{\mathbf{w}}$, temperature learning rate η^{α} $\}$

Denote network parameters by $\Psi.\theta$, $\Psi.\mathbf{w}_1$, $\Psi.\mathbf{w}_2$, $\Psi.\bar{\mathbf{w}}_1$, $\Psi.\bar{\mathbf{w}}_2$, and $\Psi.\alpha$

Initialize parameters $\Psi.\theta$, $\Psi.\mathbf{w}_1$, and $\Psi.\mathbf{w}_2$

$\Psi.\bar{\mathbf{w}}_1 \doteq \Psi.\mathbf{w}_1$; $\Psi.\bar{\mathbf{w}}_2 \doteq \Psi.\mathbf{w}_2$; $\Psi.\alpha \doteq 1$

return Ψ

Function Learn(B, Ψ):

$(\theta, \mathbf{w}_1, \mathbf{w}_2, \bar{\mathbf{w}}_1, \bar{\mathbf{w}}_2, \alpha) \doteq$

$\Psi.(\theta, \mathbf{w}_1, \mathbf{w}_2, \bar{\mathbf{w}}_1, \bar{\mathbf{w}}_2, \alpha)$

for each gradient step from 1 to g do

Sample a mini-batch M of size m uniformly randomly from B

$\mathbf{w}_1 \doteq \mathbf{w}_1 -$

$\eta^{\mathbf{w}} \frac{1}{m} \sum_{(S_k, A_k, R_{k+1}, S'_{k+1}, T_{k+1}) \in M} \nabla_{\mathbf{w}_1} L_{\mathbf{w}_1,k}$

$\mathbf{w}_2 \doteq \mathbf{w}_2 -$

$\eta^{\mathbf{w}} \frac{1}{m} \sum_{(S_k, A_k, R_{k+1}, S'_{k+1}, T_{k+1}) \in M} \nabla_{\mathbf{w}_2} L_{\mathbf{w}_2,k}$

using (3), where

$L_{\mathbf{w}_1,k} \doteq \frac{1}{2} \left(\hat{q}_{\mathbf{w}_1}(S_k, A_k) - (R_{k+1} + (1 - T_{k+1})\gamma V(S'_{k+1})) \right)^2,$

$L_{\mathbf{w}_2,k} \doteq \frac{1}{2} \left(\hat{q}_{\mathbf{w}_2}(S_k, A_k) - (R_{k+1} + (1 - T_{k+1})\gamma V(S'_{k+1})) \right)^2,$

$V(S'_{k+1}) \doteq \min \left(\hat{q}_{\bar{\mathbf{w}}_1}(S'_{k+1}, \tilde{A}_{k+1}), \hat{q}_{\bar{\mathbf{w}}_2}(S'_{k+1}, \tilde{A}_{k+1}) \right) - \alpha \log \pi_{\theta}(\tilde{A}_{k+1}|S'_{k+1}),$

and $\tilde{A}_{k+1} \sim \pi_{\theta}(\cdot|S'_{k+1}) \doteq$

$\mathcal{N}(\mu_{\theta}(S'_{k+1}), \sigma_{\theta}(S'_{k+1})^2)$

$\theta \doteq$

$\theta - \eta^{\theta} \frac{1}{m} \sum_{(S_k, A_k, R_{k+1}, S'_{k+1}, T_{k+1}) \in M} \nabla_{\theta} L_{\theta,k}$
using (2), where

$L_{\theta,k} \doteq \alpha \log \pi_{\theta}(f(S_k, \epsilon_k, \theta)|S_k)$

$- \min \left(\hat{q}_{\mathbf{w}_1}(S_k, f(S_k, \epsilon_k, \theta)), \hat{q}_{\mathbf{w}_2}(S_k, f(S_k, \epsilon_k, \theta)) \right),$

$f(S_k, \epsilon_k, \theta) \doteq \mu_{\theta}(S_k) + \epsilon_k \sigma_{\theta}(S_k),$

// reparameterization

and $\epsilon_k \sim \mathcal{N}(0, 1)$

$\alpha \doteq$

$\alpha - \eta^{\alpha} \frac{1}{m} \sum_{(S_k, A_k, R_{k+1}, S'_{k+1}, T_{k+1}) \in M} \nabla_{\alpha} L_{\alpha,k}$
using (4), where

$L_{\alpha,k} \doteq -\alpha \log \pi_{\theta}(f(S_k, \epsilon_k, \theta)|S_k) - \alpha \bar{\mathcal{H}},$

and $\bar{\mathcal{H}} \doteq -|\mathcal{A}|$

$\bar{\mathbf{w}}_1 \doteq \tau \mathbf{w}_1 + (1 - \tau) \bar{\mathbf{w}}_1$

$\bar{\mathbf{w}}_2 \doteq \tau \mathbf{w}_2 + (1 - \tau) \bar{\mathbf{w}}_2$

end

$\Psi.(\theta, \mathbf{w}_1, \mathbf{w}_2, \bar{\mathbf{w}}_1, \bar{\mathbf{w}}_2, \alpha) \doteq$

$(\theta, \mathbf{w}_1, \mathbf{w}_2, \bar{\mathbf{w}}_1, \bar{\mathbf{w}}_2, \alpha)$

return Ψ

HYPER-PARAMETERS

TABLE I

BASELINE HYPER-PARAMETERS OF PPO ON THE REACHER AND THE DOUBLE PENDULUM TASKS.

baseline hyper-parameters	value
b	2000
m	50
γ	0.99
λ	0.95

TABLE II

TUNED HYPER-PARAMETERS OF PPO ON THE REACHER TASK.

tuned hyper-parameters	δt (ms)				
	4	8	16	32	64
b	8000	8000	4000	2000	1000
m	50	25	12	12	12

TABLE III

BASELINE AND δt -AWARE HYPER-PARAMETERS OF PPO ON REACHER AND DOUBLE PENDULUM TASKS.

hyper-parameters		value
baseline	δt -aware	
b	b_{16}	2000
m	m_{16}	50
γ	γ_{16}	0.99
λ	λ_{16}	0.95

TABLE IV

TUNED γ OF SAC ON THE REACHER TASK.

tuned hyper-parameter	δt (ms)				
γ	4	8	16	32	64
γ	0.961	0.923	0.851	0.851	0.851

TABLE V

HYPER-PARAMETERS OF PPO ON THE REAL-ROBOT REACHER TASK.

hyper-parameters		value
baseline	δt -aware	
b	b_{40}	400
m	m_{40}	10
γ	γ_{40}	0.99
λ	λ_{40}	0.95

ADDITIONAL FIGURES

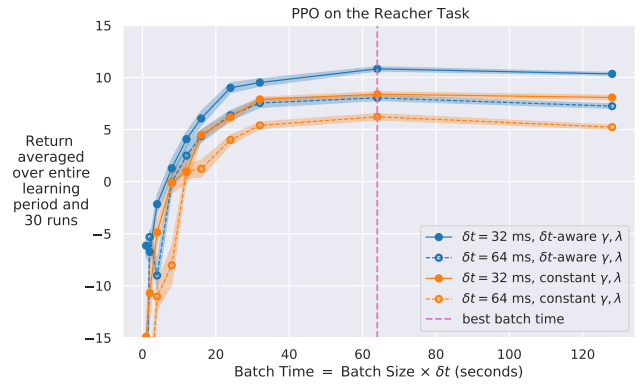


Fig. 12. Overall average return of δt -aware hyper-parameters compared with ones where $\gamma_{\delta t} = \gamma_{16} = 0.99$ and $\lambda_{\delta t} = \lambda_{16} = 0.95$ are constant in all runs (constant).

PPO on the Reacher Task

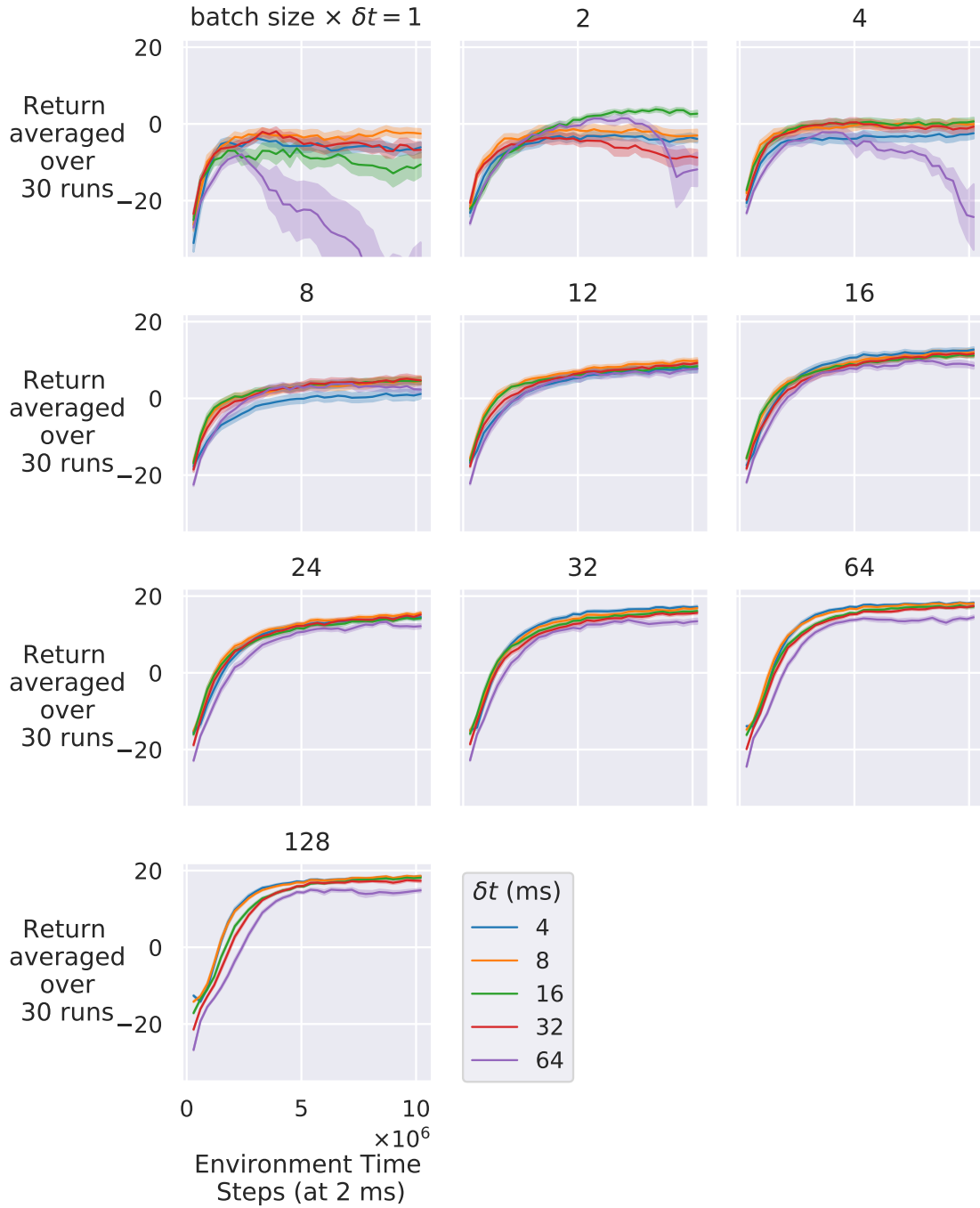


Fig. 13. Corresponding learning curves for Figure 3 using the δt -aware hyper-parameters. Performance improves with increasing batch times for all cycle times.

PPO on the Reacher Task

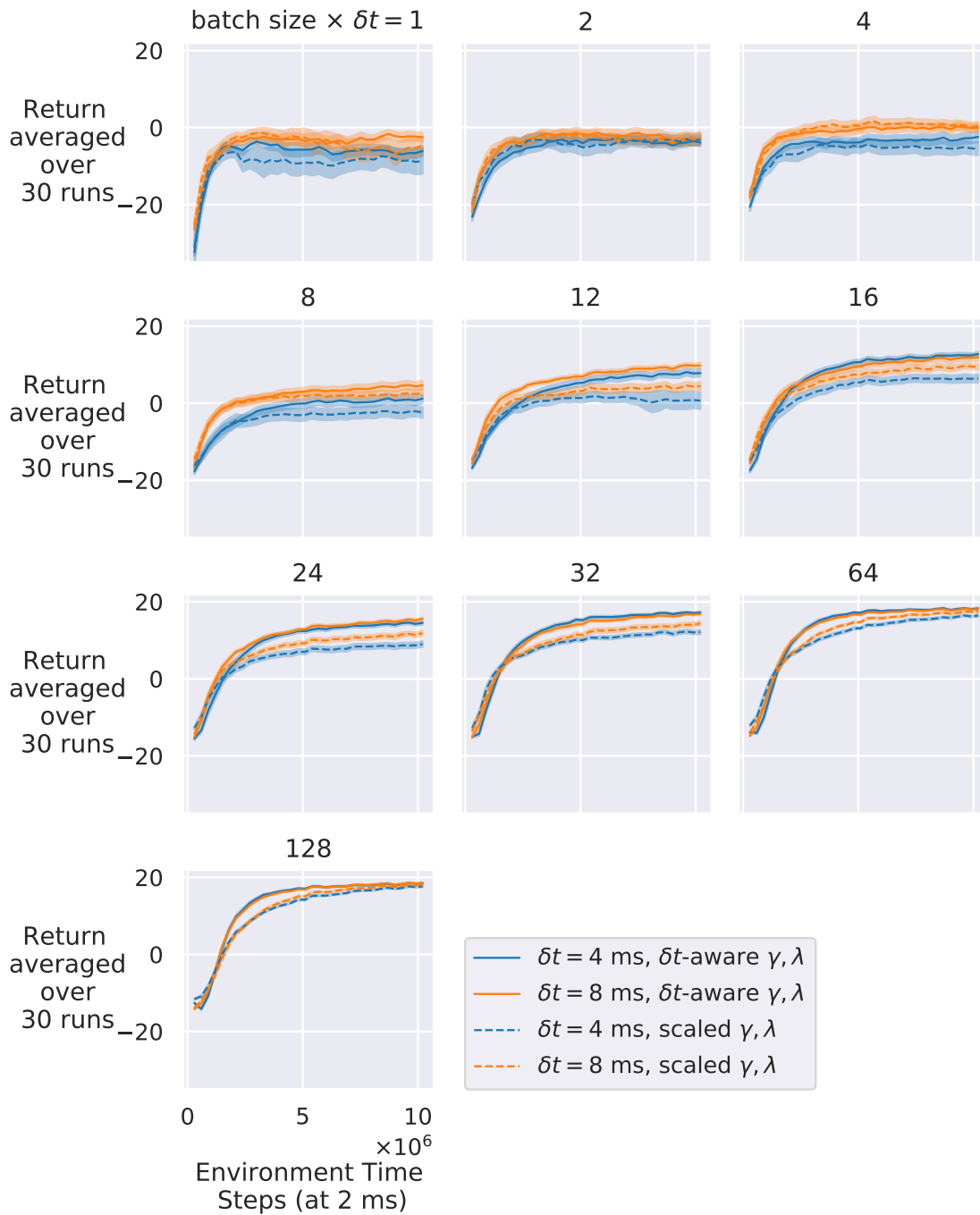


Fig. 14. Corresponding learning curves for Figure 4 comparing the δt -aware hyper-parameters with ones where the discount factor γ and trace-decay parameter λ are always exponentiated to the $\delta t/\delta t_0$ power (scaled). Only the $\delta t = 4$ ms and $\delta t = 8$ ms curves are plotted since the rest are similar to Figure 13.

PPO on the Reacher Task

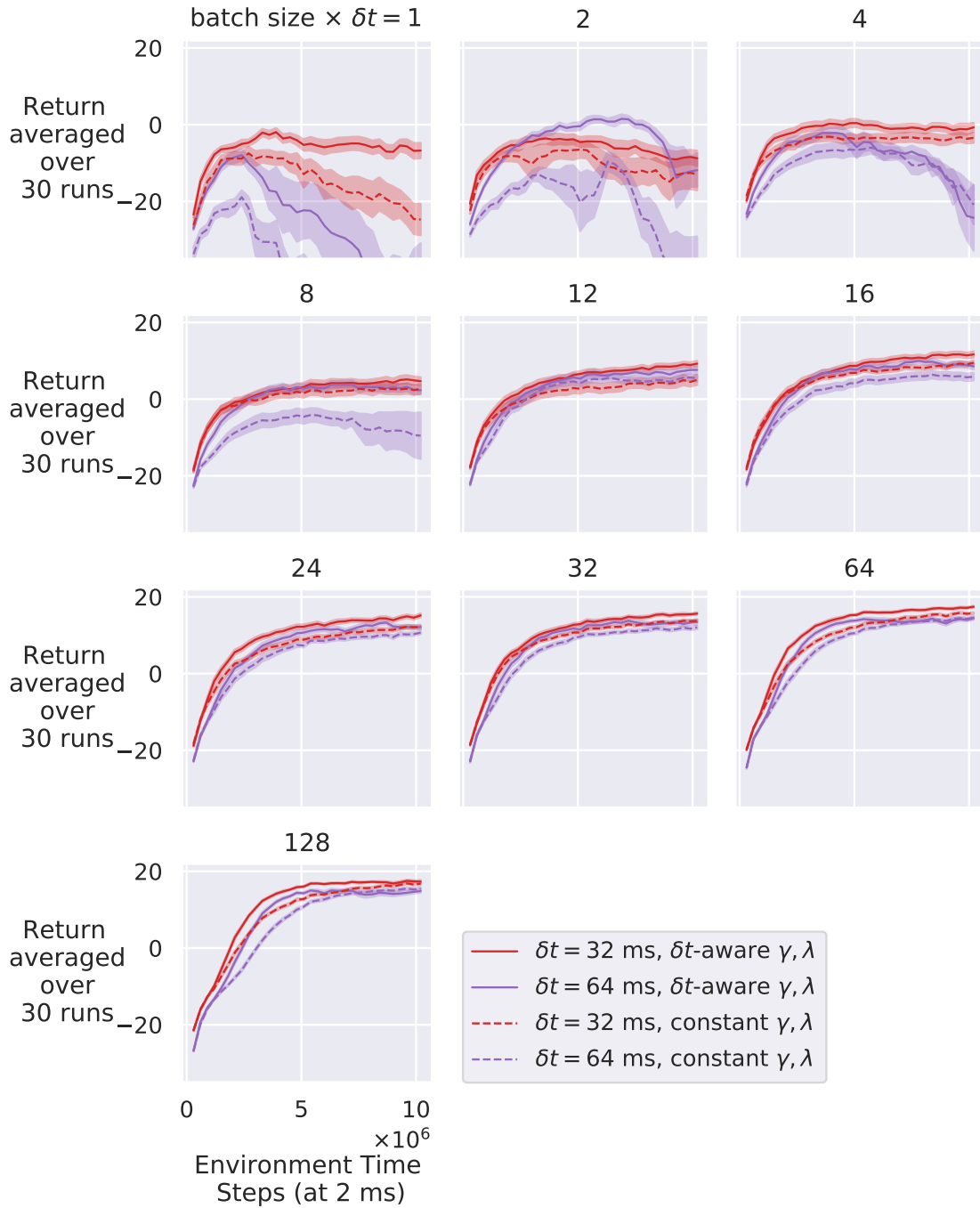


Fig. 15. Corresponding learning curves for Figure 12 comparing the δt -aware hyper-parameters with ones where the discount factor $\gamma_{\delta t} = \gamma_{16} = 0.99$ and trace-decay parameter $\lambda_{\delta t} = \lambda_{16} = 0.95$ are constant in all runs (constant). Only the $\delta t = 32$ ms and $\delta t = 64$ ms curves are plotted since the rest are similar to Figure 13.

SAC on the Reacher Task

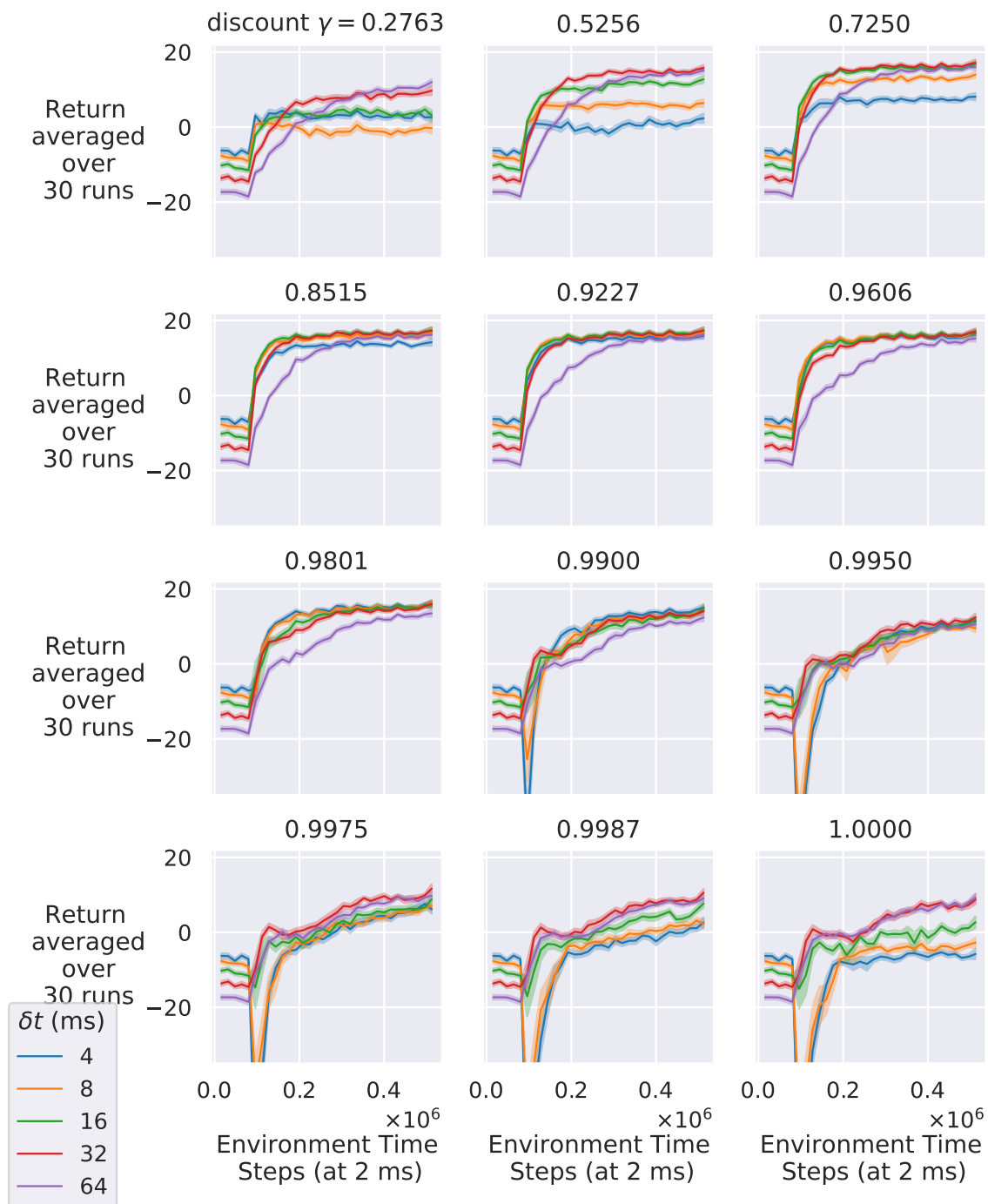


Fig. 16. Corresponding learning curves of SAC for Figure 7 for a sweep of γ values. Intermediate values of γ obtain better asymptotic performance and learning speed.

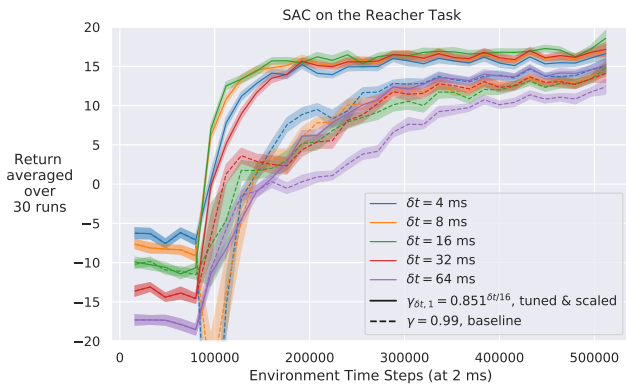


Fig. 17. Corresponding learning curves of SAC for Figure 8 (left) comparing the baseline with the tuned and scaled $\gamma_{\delta t,1} = 0.851^{\delta t/16}$. All cycle times learn faster and avoid the sharp drops of smaller cycle times with the baseline γ .

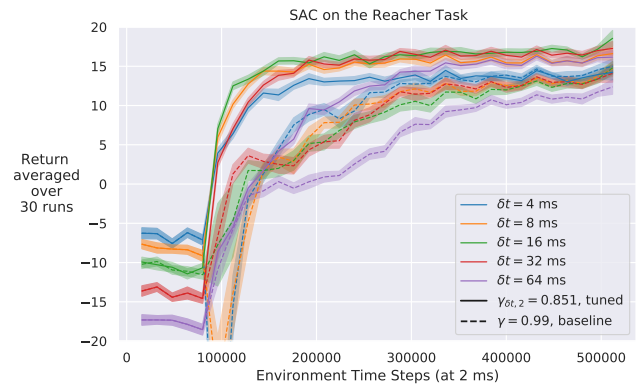


Fig. 18. Corresponding learning curves of SAC for Figure 8 (left) comparing the baseline with the tuned $\gamma_{\delta t,2} = 0.851$. All cycle times learn faster and avoid the sharp drops of smaller cycle times with the baseline γ .

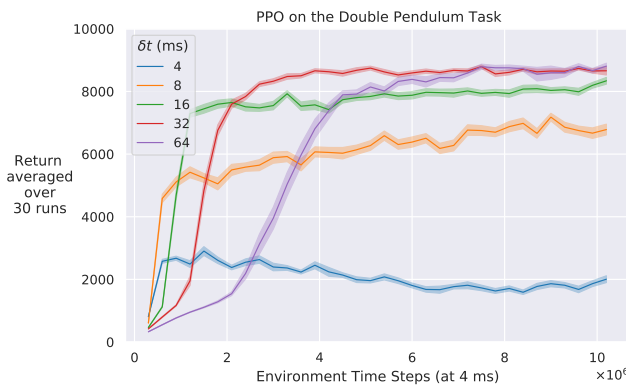


Fig. 19. Corresponding learning curves of PPO for Figure 8 (middle) using the baseline hyper-parameters on the Double Pendulum Task. Different cycle times vary greatly in asymptotic performance and learning speed.

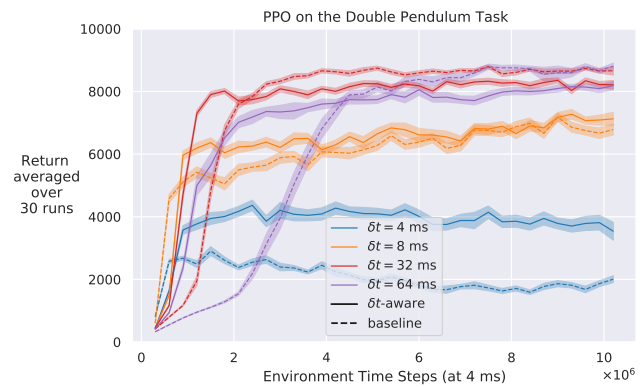


Fig. 20. Corresponding learning curves of PPO for Figure 8 (middle) comparing the baseline and δt -aware hyper-parameters on the Double Pendulum Task. With the δt -aware hyper-parameters, different cycle times are more similar in asymptotic performance and learning speed.

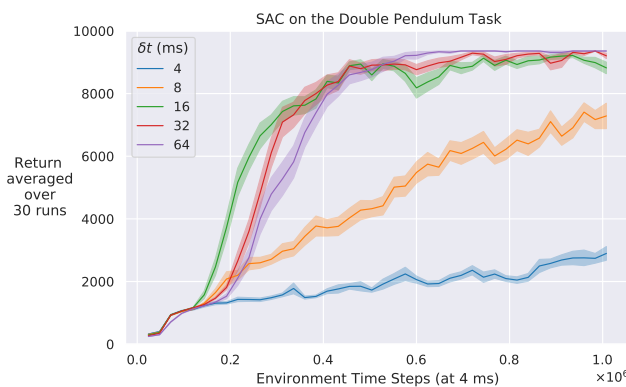


Fig. 21. Corresponding learning curves of SAC for Figure 8 (right) using the baseline γ . Learning speed of smaller cycle times is significantly impaired, and they seemingly could not reach their asymptote in the time given.

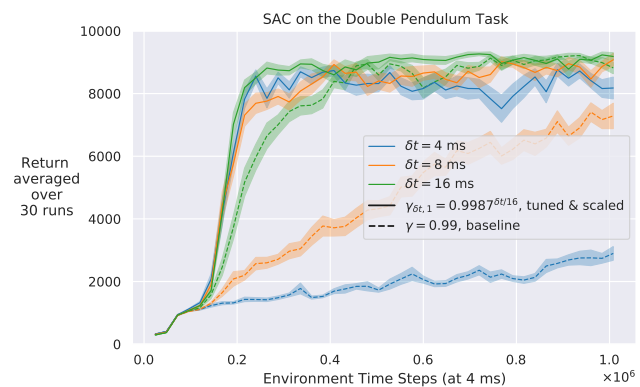


Fig. 22. Corresponding learning curves of SAC for Figure 8 (right) comparing the baseline with the tuned and scaled $\gamma_{\delta t,1} = 0.9987^{\delta t/16}$. Performance of smaller cycle times is recovered. Larger cycle times were not drawn since no major change was observed compared to the baseline γ .

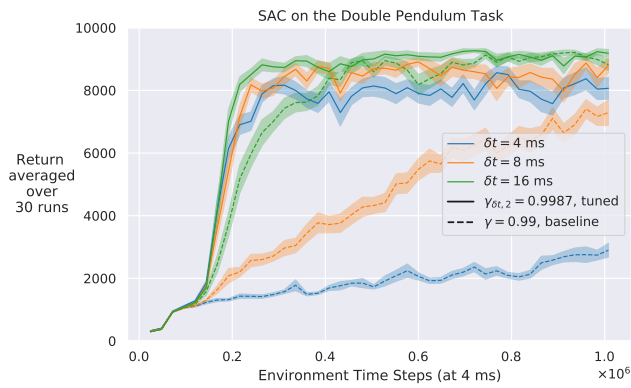


Fig. 23. Corresponding learning curves of SAC for Figure 8 (right) comparing the baseline with the tuned $\gamma_{\delta t, 2} = 0.9987$. Performance of smaller cycle times is recovered. Larger cycle times were not drawn since no major change was observed compared to the baseline γ .

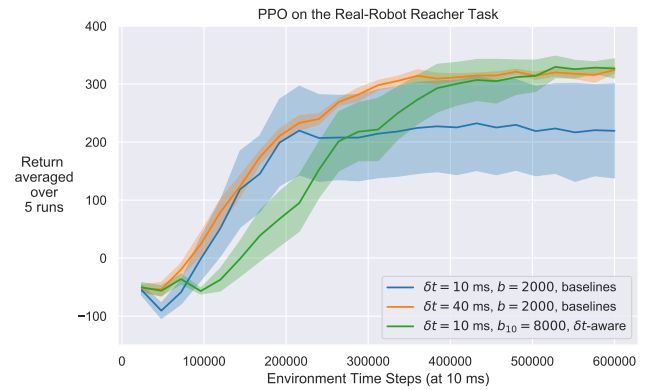


Fig. 24. Learning curves of PPO on the Real-Robot Reacher Task comparing the δt -aware and baseline hyper-parameters of Table III. Performance of $\delta t = 10$ ms and $\delta t_0 = 40$ ms are comparable with the baseline hyper-parameters.

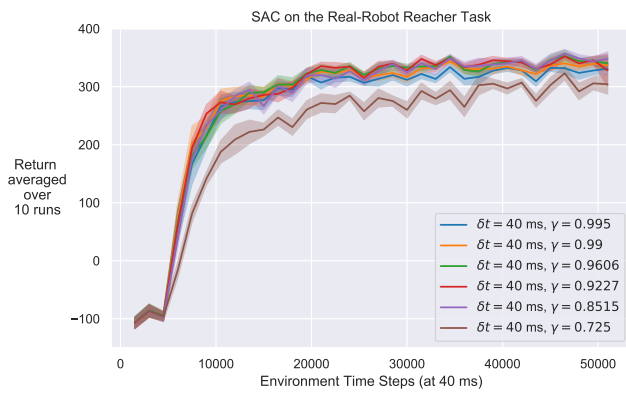


Fig. 25. Corresponding learning curves of SAC for Figure 11 on the Real-Robot Reacher Task for the sweep of γ values at $\delta t_0 = 40$ ms. The smallest $\gamma = 0.725$ performs slightly worse than other γ s. Other γ s are roughly similar in learning speed and asymptotic performance.

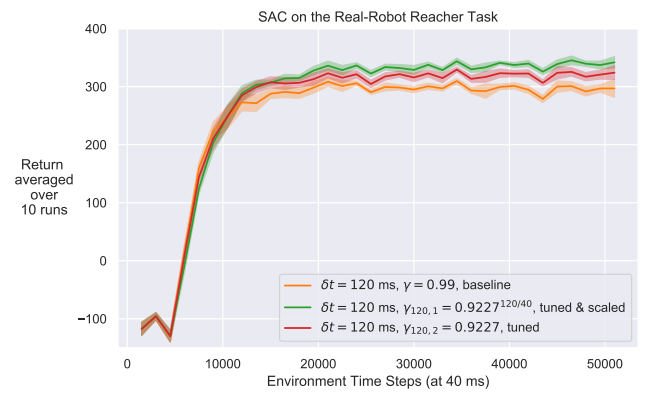


Fig. 26. Corresponding learning curves of SAC for Figure 11 on the Real-Robot Reacher Task for $\delta t = 120$ ms. The asymptotic performance of the baseline $\gamma = 0.99$ cannot reach that of the atypical δt -aware $\gamma_{\delta t, 1} \approx 0.786$ even after extended learning.